

Factors Affecting ENF Capture in Audio

Adi Hajj-Ahmad, Chau-Wai Wong, Steven Gambino, Qiang Zhu, Miao Yu, and Min Wu

Abstract—The Electric Network Frequency (ENF) signal is an environmental signature that can be captured in audio and video recordings made in locations where there is electrical activity. This signal is influenced by the power grid in which the recording is made, and recent work has shown that it can be useful towards a number of forensics and security applications. Most of the previous work done on the ENF signature can be categorized into two groups: work that targets improving approaches to extract the ENF signal, and work that explores applications that the ENF signature can be used for. An under-studied area of ENF research is the factors that can affect the capture of ENF traces in media recordings. Indeed, not all recordings made in areas of electrical activity will carry prominent ENF traces, and the strengths by which the ENF traces are captured can vary from one recording to another. A thorough understanding of the factors that can affect the capture of ENF traces in recordings is essential to understanding the true applicability of ENF-based approaches and can help inform future related studies. In this paper, we carry out a study on such factors, with a focus on audio signals, where we provide an overview of factors discussed earlier in the literature and examine new ones. We conclude with outlining avenues for future work.

Index Terms—ENF traces, embedding, recording environment, recording devices.

EDICS Category: MMF-BENM-PER (Performance measurement and validation of forensic evidence)

I. INTRODUCTION

MOST of the power provided by power grids comes from turbines that work as generators of alternating current. The rotational velocity of these turbines determines the Electric Network Frequency (ENF), which typically has a nominal value of 60 Hz in most of the Americas, and 50 Hz in most other parts of the world. The ENF fluctuates around its nominal value as a result of power-frequency control mechanisms that maintain the balance between generation and consumption of electric energy across the grid [1]. These fluctuations are seen as random, unique in time, and are typically very similar in all locations of the same grid. The changing instantaneous value of the ENF over time is what we define as the *ENF signal*.

The manuscript was submitted on October 18, 2017, revised on February 21, 2018 and April 13, 2018, and accepted for publication on April 17, 2018. The associate editor coordinating the review of this manuscript and approving it for publication was Prof. Xinpeng Zhang. The work shown in this paper was carried out when all authors were with UMD (University of Maryland, College Park, MD). This work was supported by the National Science Foundation (NSF) under Grants 1309623 and 1320803. A. Hajj-Ahmad is with General Electric in San Ramon, CA (e-mail: adi.hajj-ahmad@ge.com); C.-W. Wong is with the Department of Electrical and Computer Engineering, North Carolina State University (e-mail: chauwai.wong@ncsu.edu); S. Gambino and M. Yu are with UMD's Department of Mechanical Engineering (e-mails: lekua47@terpmail.umd.edu, mmyu@umd.edu); Q. Zhu and M. Wu are with UMD's Department of Electrical and Computer Engineering (e-mails: zhuqiang@umd.edu and minwu@umd.edu).

ENF traces can be captured by audio or video recordings made in areas where there is electrical activity. This makes the ENF signal particularly relevant to information forensics as it allows the ENF signal to serve as an environmental signature that is intrinsically embedded in media recordings. Several approaches have been proposed to extract the ENF signal from media recordings, including approaches based on the use of the Short Time Fourier Transform (STFT) and subspace-based approaches such as MUSIC and ESPRIT [2]–[4]. Once the ENF signal is extracted, it can be used for a number of forensics applications, such as time and location-of-recording authentication/identification and tampering detection [2], [5]–[9].

Similar to [10]’s categorization on existing works on the ENF, we find that the majority of the past research into the ENF signature has largely focused on two areas: developing or improving approaches to accurately extract the ENF signal from media recordings [3], [11]–[16], and examining novel ENF-based applications or improving on their performance [5]–[9], [17]–[20]. Amid all this work towards extracting and using the ENF signature, an essential research question remains without a solid answer: In what kind of recording situations can we be confident that ENF traces will be captured in media signals? Answering this question can be informative to the true applicability of the ENF signature, and can be beneficial towards the development and deployment of ENF-based applications.

The ENF traces are an imprint of power grid activity on media recordings, so a basic requirement for the capture of ENF traces is that there should be some sort of electrical activity in the place of recording. A distinction can be made between two types of recordings: recordings made using recorders connected to the power mains and recordings made using battery-powered recorders. In the case of the former, it is generally accepted that ENF traces will appear in the resultant recording, due to electromagnetic interference resulting from the recorder’s connection to the power mains [21]. It is in the case of the latter that the situation becomes more complex.

In this paper, we carry out a study exploring factors that can affect the capture of ENF traces in media recordings. Our focus here is on *audio* recordings made using *battery-powered* recorders. First, we summarize results in the literature that have addressed this issue. Next, we examine further factors that can promote or hinder the capture of ENF traces. Our explorations include two types of factors: (1) those related to the recording environment and (2) those related to the recording device used.

The rest of this paper is organized as follows. In Section II, we present a summary on the results of the studies previously done towards understanding the factors affecting the capture of ENF traces in audio recordings. In Sections III and IV,

TABLE I
SAMPLE OF FACTORS AFFECTING THE CAPTURE OF ENF TRACES IN
AUDIO RECORDINGS MADE BY BATTERY-POWERED RECORDERS

Factors	Effect
Environmental	Electromagnetic (EM) fields Promote ENF capture in recordings made by <i>dynamic</i> microphones but not in those made by <i>electret</i> microphones.
	Acoustic mains hum Promotes ENF capture; sources include fans, power adaptors, lights, and fridges.
	Electric cables in vicinity Not sufficient for ENF capture.
Device-related	Microphone type Different types have different reactions to the same sources, e.g., to EM fields.
	Frequency band of recorders Recorder may be incapable of recording low frequencies, e.g., around 50/60 Hz.
	Recorder internal compression Strong compression, e.g., Adaptive Multi-Rate, can limit ENF capturing.

we present our explorations into the effect of the recording environment and the recording device, respectively, on the capture of ENF traces. In Section V, we conclude the paper and outline avenues for future work.

II. OVERVIEW OF PREVIOUS WORK

Understanding the factors that promote or hinder the capture of ENF traces in media recordings can help towards gaining a stronger understanding on the situations in which ENF analysis is applicable. It can also inform the way in which ENF-based applications are developed. In this section, we summarize results shown in previous studies pertaining to the factors affecting the capture of ENF traces in audio recordings made by battery-powered recorders.

Table I shows a sample of factors that have been studied in the literature for their effect on the capture of ENF traces in audio recordings [21]–[23]. As shown, broadly speaking, the capture of ENF traces can be affected by several factors that can be divided into two categories: factors related to the environment in which the recording was made and factors related to the recording device used to make the recording. Interaction between different factors may as well lead to different results. For instance, as can be seen in Table I, electromagnetic fields in the place of recording promote the capture of ENF traces if the recording microphone is *dynamic* but not in the case where this microphone is *electret*.

Overall, the most common cause of the capture of ENF traces in audio recordings is the acoustic mains hum, which can be produced by mains-powered equipment in the place of recording. Recently, the hypothesis that this background noise is a carrier of ENF traces was confirmed in [21]. Experiments carried out in an indoor setting suggested a high robustness of ENF traces. These traces were present in a recording made 10 meters away from a noise source emitting ENF-containing noise and located in a different room.

In general, ENF traces are not restricted to appear in the frequency band surrounding the nominal 50/60 Hz band, but can also appear in bands surrounding the higher harmonics of the nominal ENF value, i.e., around integer multiples of 50/60 Hz. When examining signals containing ENF traces, it is common to observe scaled versions of almost the same

variations appearing at different harmonic frequencies. The specific harmonics at which the ENF traces appear and the strength of the captured traces at each harmonic may differ from one recording to another [11], [12]. Therefore, the locations and corresponding strengths by which the ENF traces appear should be considered as well when examining factors affecting the capture of ENF traces in media.

In the following sections, we present our explorations on factors that may influence the embedding of ENF traces in audio recordings due to the environment in which the recording was made and due to the recording device being used.

III. EXPLORATIONS ON ENVIRONMENT-RELATED FACTORS

As established in Section II, a main source of ENF traces in audio recordings is the acoustic mains hum. Knowing this, it can be useful to examine the way in which the acoustic mains hum can behave as a physical sound wave in a recording environment [24]. This can help understand its effects on the manner in which ENF traces are embedded in an audio recording.

The acoustic mains hum is a sound signal, and sound is a mechanical longitudinal wave. It is a disturbance that travels through a medium, transporting energy from one location to another through a series of interacting particles. It is a longitudinal wave because the particles, e.g., air molecules, vibrate in a direction parallel to the direction of propagation of the wave. The sound wave can then be characterized by compressions and rarefactions, which are physical regions where particles are compressed together and regions where particles are spread apart, respectively. Sound waves move at a speed c that depends on the medium in which they travel. A sound wave can generally be characterized by its frequency f and wavelength λ , which can be related to each other through the wave speed equation: $c = f \cdot \lambda$.

The acoustic mains hum can be seen as the summation of several sound waves of varying strengths (amplitudes) at frequencies that are multiples of the nominal ENF value. Using the speed of sound in air at 20°C (343 m/s) and the wave speed equation, we find that the wavelengths of sound waves at different ENF harmonics would range in value from 0.8 m to 7 m. This helps put in perspective the movement of these sound waves in a location where we expect an audio recording to capture ENF traces.

In the remainder of this section, we show results on experiments done in different environment conditions that demonstrate how the factors related to the recording environment can affect the way the ENF traces are captured in a recording.

A. Effect of wave interference

In this section, we demonstrate that the specific location in a room in which a recorder is placed may have an effect on the strength of the ENF traces captured in the resulting recording. The factor we investigate in this case is the effect of wave interference; in particular, the interference of sound waves carrying ENF traces.

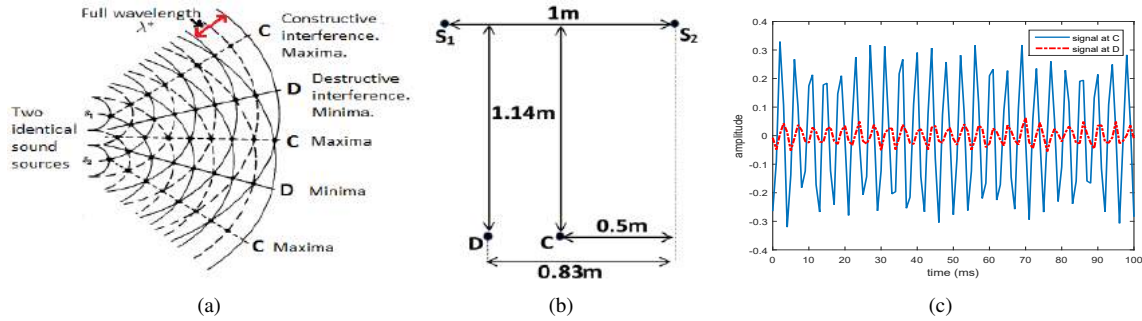


Fig. 1. (a) is a diagram showing the result of interference of two identical sound waves. Original image (before modification) from [25]. (b) shows a schematic of the set-up for the sound wave interference experiment we carried out; S_1 and S_2 denote the locations of the speakers emitting the sound waves; C and D denote the locations where Olympus recorders are placed to pick up constructive and destructive interferences, respectively. (c) shows samples of the audio signals recorded at locations C and D .

In a given location where there are equipment connected to the power mains, the acoustic mains hum may be emitted from different sources. Behaving as sound waves, the multiple versions of this signal, along with their reflections, would lead to various levels of interference in the location. The two extremes of these interferences are the *constructive* interference and the *destructive* interference.

Figure 1(a) shows a diagram of how waves emitted from two point sources are expected to interfere with each other. In this diagram, two sources are emitting identical signals of wavelength λ^* , which is the distance between any two solid curves, or any two dotted curves. Locations of expected constructive and destructive interference can be seen in the figure denoted by C 's and D 's, respectively. Constructive interference is created in locations where compressions from the two signals meet, creating an area of even higher pressure, followed by a meeting of rarefactions from the two signals, making the pressure in the area even lower. The overall effect is that the combined signal becomes stronger. Destructive interference is the opposite of constructive interference. It occurs at locations where a compression meets a rarefaction, thereby canceling each other out and resulting in little movement of the medium's particles.

Viewing the signals of Figure 1 as sound waves carrying ENF traces, this suggests that in certain environments where ENF traces are expected to occur, e.g., a room where there is electrical activity, ENF traces may not appear in a recording made in this environment or may appear at different strengths depending on the specific location of the recorder within the environment. We carried out a verification experiment to observe this phenomenon in a controlled setting. We generated a synthetic tone signal at 240 Hz and emitted it from two speakers placed 1 m apart. Figure 1(b) shows the layout we used. We placed two recorders of the same brand, Olympus 700-M audio recorders [26], one at a central location C expected to exhibit constructive interference, and one at another location D expected to exhibit destructive interference.

We show samples of the recorded audio signals in Figure 1(c). Although the signal recorded at location D in theory should be a zero signal, the presence of a non-negligible amplitude can be explained by somewhat constructive interference from reflected versions of the original two signals.

It could also be due to the non-ideal point source condition in the experiment. In a more controlled recording setting, the amplitude of the signal recorded at D should be much lower. However, we can see that the signal recorded at location C is stronger, i.e., has a larger amplitude of around 0.25, than the signal recorded at location D , which has a lower amplitude of around 0.03. This is consistent with what we would expect given our understanding of sound wave interference.

In a practical scenario where a recorder is recording an acoustic signal carrying ENF traces, there may be several sources in the room emitting signals carrying ENF traces, and some of these signals will be reflected as well. All these signals will interfere with one another to form the signal recorded by the recorder. The discussions in this section suggest that the particular location of the recorder within the place of recording will have an effect on how the ENF traces are captured.

B. Effect of recorder movement

In this section, we demonstrate that moving a recorder while carrying out a recording can have an adverse effect on the quality of the captured ENF traces in the resulting recording.

a) *Casual Walk*: We carried out an experiment where we made a 10-min audio recording using an Olympus recording in an office setting in Maryland, where the nominal ENF value is 60 Hz. The Olympus recorder was stationary during the first half of the recording and then was continuously moved during the second half of the recording. During the movement period, the person carrying out the recording was carrying the recorder and moving it around by hand in a random manner while casually walking around in a room. Figure 2(a) shows the spectrogram strips about the ENF harmonics for the recorded signal. We can see that, along with ENF traces around the 120 Hz and 240 Hz harmonics, there is a prominent ENF trace around the 360 Hz harmonic in the first half of the signal. After the 5-minute mark, however, the ENF traces become distorted and indistinguishable.

While recording the audio recording, we had concurrently recorded a 10-min *reference power recording*. This recording is made using another Olympus recorder connected to a power outlet using a step-down transformer and a voltage divider circuit [2], [27]. This set-up allows the resulting recording to

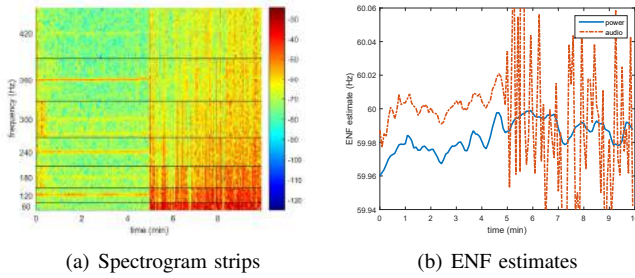


Fig. 2. (a) Spectrogram strips about the harmonics of 60 Hz from an audio recording where the recorder starts moving at the 5-min mark, and (b) ENF signals extracted from the audio recording and a simultaneously recorded reference power recording.

carry ENF traces at a high signal-to-noise ratio (SNR). As this reference recording is made concurrently with the audio recording, the fluctuations in the ENF values observed in both recordings should be very similar. In this way, the ENF traces extracted from the reference power recording can serve as a guide towards understanding how well the ENF traces appear in the audio recording.

Figure 2(b) shows the ENF signal extracted from the audio recording (from around the 360 Hz component) and the ENF signal extracted from the simultaneously recorded reference power recording. We can see that the audio ENF signal matches well with the power signal in the first 5 minutes, but not afterwards, which is when the audio recorder was being moved. The correlation coefficient between the audio and power ENF signals was as high as 95% in the first half of the recording.

This experiment demonstrates that moving the audio recorder while a recording is being made can affect the quality of the captured ENF traces. One possible explanation for the cause behind this observation is air pressure fluctuations. Most microphones will suffer from air pressure fluctuations during movement. This would result in significant noise that could also affect the capture ENF traces. Another possible factor for explaining the change in the frequency of the captured ENF traces is the Doppler effect. We explore this further through the controlled experiments in the next subsection.

b) Controlled Movement: The Doppler effect relates the observer's frequency f with the speed of the observer moving toward the source v_r and the source frequency f_0 as follows

$$f = \left(1 + \frac{v_r}{c}\right) f_0 \quad (1)$$

where c is the speed of the propagation of the wave. Here, we conducted a controlled experiment using a synthetic constant frequency source as reported below to examine if the Doppler effect can be observed in recordings of a moving audio recorder.

We carried out a 9-min controlled experiment with a *motion segment* (3–6 min) during which a person holds the recorder walking at a constant speed towards and away from the source, and two *still segments* (0–3 min and 6–9 min) during which the recorder was placed on a table. The source is a speaker playing a 55 Hz artificially generated single tone sound. During the motion segment, the person walked away from the source nine

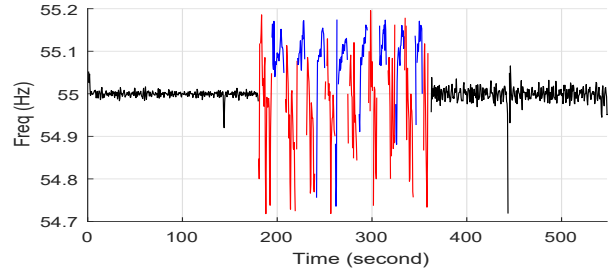


Fig. 3. Estimated dominating frequencies over time for the recording made in the controlled experiment on verifying the Doppler effect of a moving audio recorder. Still segments: 0–3 min and 6–9 min, in black. Motion segment: 3–6 min. The highlighted blue and red portions correspond to motions facing and moving away from the source.

times and walked towards it eight times. Figure 3 shows the frequency of the captured sound estimated with a 2-second sliding window and 90% overlap. The plot clearly shows, in blue and red, 17 different sub-segments of the motion segment (3–6 min) with alternating frequencies around the source frequency, which correspond to the motions toward (blue) and away from (red) the source. The plot also shows that there is no significant frequency change in the still segments. Compared to the red segments during which the recorded signal was partially blocked by the tester when walking away from the source, the blue segments show a repeatable pattern that the frequency was increased to a range of [55.05, 55.15] Hz. When the Doppler effect is used to explain such change, it corresponds to a moving speed in a range of [0.31, 0.93] m/sec. The ground-truth moving speed obtained from a separate video recording of the scene of the experiment was 0.46 m/sec. The above results suggest that a substantial part of the frequency change is related to the Doppler effect characterized by (1).

We then designed more practical factor-controlled experiments as listed in Table II: EXP. 2 to EXP. 6 test the effect of motions from small to large scale; EXP. 7 and EXP. 8 test the effect of putting recorders in pockets of pants.

Figure 4(a) is a spectrogram of a 24-min audio recording that contains one realization for each experiment from EXP. 1 to EXP. 8. Figure 4(b) shows the extracted frequency signal from the strongest harmonics at 120 Hz and uses the power signal as the reference. The extracted signal in EXP. 7 matches well with the reference power signal, indicating that putting the recorder in pockets of pants of a still person does not affect

TABLE II
DETAILED EXPERIMENTAL CONDITIONS

Exp. No.	Time (min)	Motion conditions
1	0–3	Recorder kept still on table
2	3–6	Random motion, handheld in 1-m ³ cube
3	6–9	Periodic back and forth, walk in 1-meter range
4	9–12	Periodic back and forth, walk in 2-meter range
5	12–15	Periodic back and forth, walk in 3-meter range
6	15–18	Periodic back and forth, walk in 4-meter range
7	18–21	Recorder kept still in left pocket of pants
8	21–24	Recorder in pocket of pants, random walk on 1-m ² plane

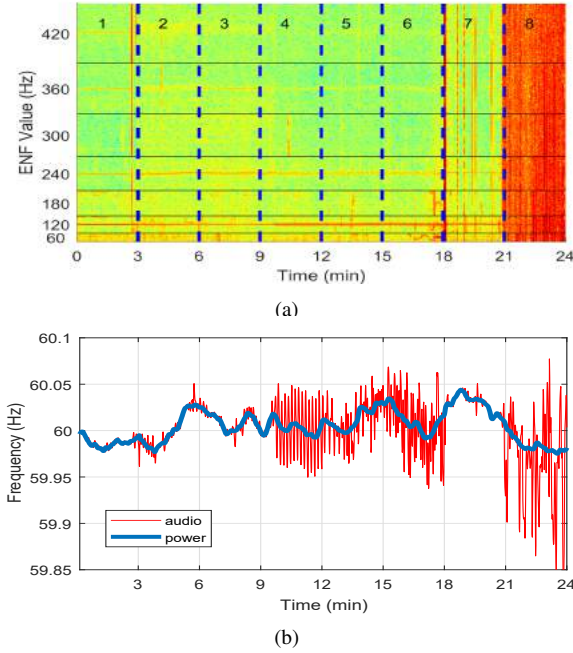


Fig. 4. (a) Spectrogram of a 24-min audio recording that contains 8 different experimental conditions listed in Table II. (b) Extracted frequency signal around 120 Hz (normalized to 60 Hz) and the power reference signal.

the quality of the acquired ENF signals. However, the contrast in spectrogram between EXP. 7 and EXP. 8 implies that putting the recorder in pockets of pants while walking can make the ENF extraction impossible due to the dominating wideband noise.

Spectrograms for EXP. 1 to EXP. 6 with different levels of motions show significant frequency traces in some ENF bands. Figure 4(b) reveals that for experiments with no motion and small motions, i.e., EXP. 1–EXP. 3, the extracted signals closely match with the reference power signals. For experiments with larger displacements, i.e., EXP. 4–EXP. 6, the extracted frequency signals fluctuate but generally have the same trend as the reference power signals.

We repeat EXP. 1, 3, 4, and 6 five times each to ensure that such observations are not by chance, and to explore the possible causes for such fluctuations. One representative plot for each experiment with extracted ENF signals and power references is shown in Figure 5. For EXP. 3, 4, and 6 that involve moving the recorder, it is observed that they have significant frequency fluctuations around the reference signal, whereas the still cases do not. Taking Figure 5(b) as an example, and using $60 + 0.015/2 = 60.0075$ Hz as the observer's maximum frequency, one can calculate the maximum speed of the observer to be $\hat{v}_r = 343 \text{ m/sec} \times (60.0075/60 - 1) = 4 \text{ cm/sec}$. Note that the actual peak-to-peak frequency variation can be greater than 0.015 Hz as any frequency value obtained from the spectrogram is the averaged frequency from an 8-sec window, long enough to cover a whole moving period. Therefore, the true maximum speed should be at least 4 cm/sec, which matches the speed in our experimental setup. Similarly, Figures 5(c) and 5(d) for the periodic walk show that the extracted ENF signals

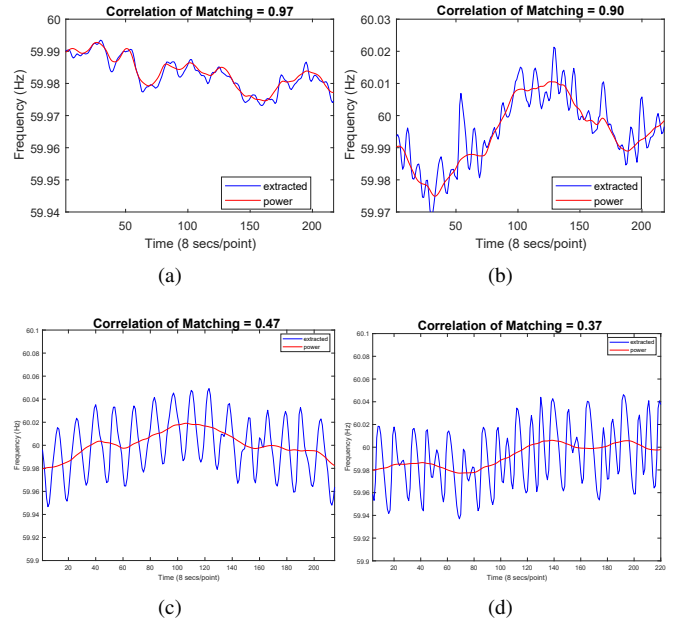


Fig. 5. Representative ENF patterns when recorder in various motion conditions. (a) EXP. 1 [still]. Peak-to-peak variation, $A_{p2p} \approx 0.0025$ Hz. (b) EXP. 3 [1-m periodic]. $A_{p2p} \approx 0.015$ Hz $\Rightarrow \hat{v}_r \geq 4 \text{ cm/s.}$ (c) EXP. 4 [2-m periodic]. $A_{p2p} \approx 0.07 \text{ Hz} \Rightarrow \hat{v}_r \geq 20 \text{ cm/s.}$ (d) EXP. 6 [4-m periodic]. $A_{p2p} \approx 0.08 \text{ Hz} \Rightarrow \hat{v}_r \geq 23 \text{ cm/s.}$

from the audio recordings have 0.07 and 0.08 Hz peak-to-peak fluctuation around the reference signal, respectively. Applying the Doppler model, we estimate that the true maximum speed of the recorder movement should be at least 20 and 23 cm/sec, respectively, which match the experimental conditions.

These factor-controlled experiments reveal that moving the recorder can affect the ENF via the Doppler effect, possibly in conjunction with other sources such as air pressure, air flow, and other vibrations. If the recorder is oscillating around the same physical location, the captured signal will be perturbed but will be around the true ENF. Overall, moving a recorder while making a recording can have an adverse effect on the quality of the ENF traces being captured. As this would add challenges to the subsequent ENF-based forensic applications, this issue should be given proper attention in practice through, for example, applying appropriate compensations or denoising techniques to the raw ENF traces.

C. ENF traces across different locations

In what follows, we aim to demonstrate and visualize how the strength of captured ENF traces can change across the length of a recording as the recording location is being changed. To this end, we use an Olympus recorder to make a single 1-hour long recording, where the recorder is moved every 2 minutes to a new location. While making this 1-hour long audio recording, we concurrently record a 1-hour long reference power recording. As seen in Section III-B, such a reference recording can serve as a guide towards understanding how well the ENF traces appear in the audio recording.

While making the audio recording, the Olympus recorder was moved to 25 different locations in the second floor

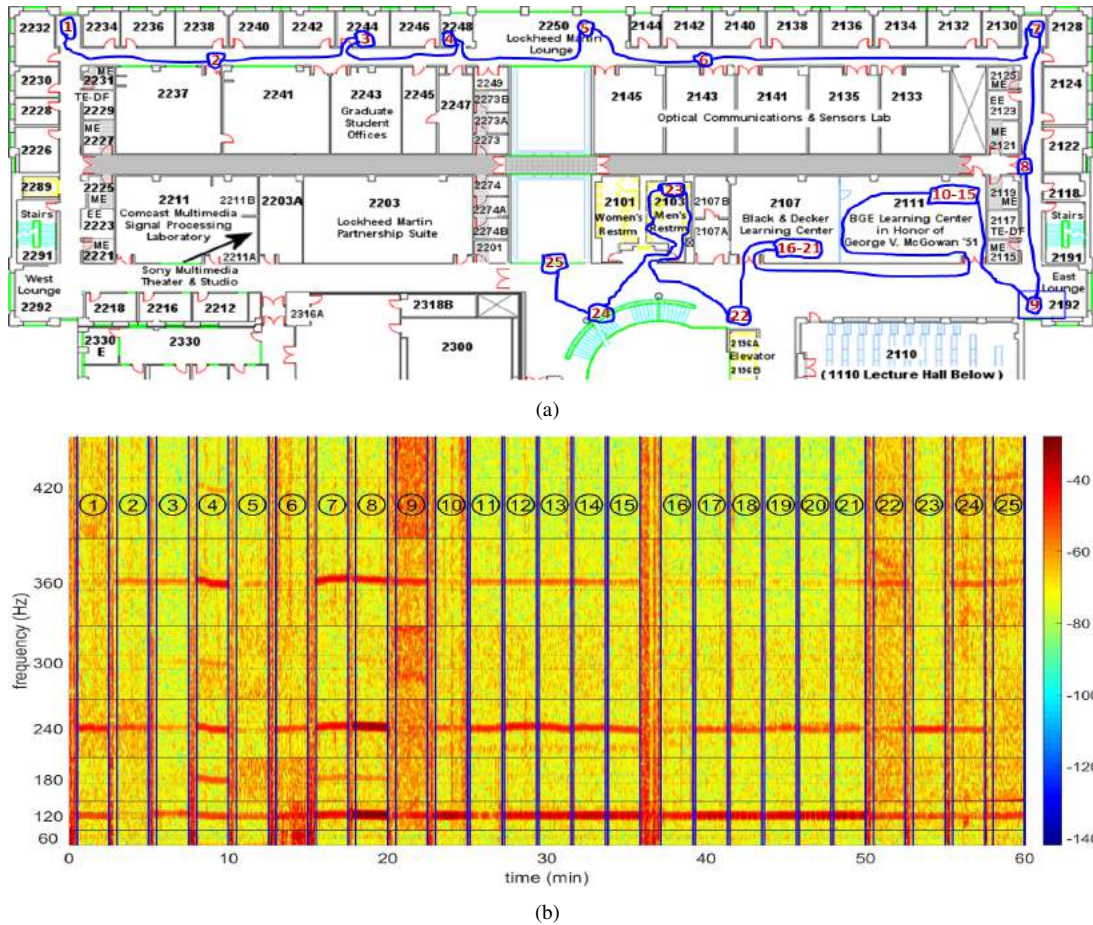


Fig. 6. (a) Floor plan of 2nd floor in KEB showing trajectory of recorder and stops made while recording. Each number denotes a 2-minute stop for the recorder. Original map obtained from [28], and (b) Spectrogram strips about ENF harmonics for the obtained 1-hour long recording. The numbers denote the location of the recorder while the recording was being made. Stops 10-15 were in the same room, and Stops 16-21 were in the same room. The blue vertical lines denote the separation between the recorder being placed in a certain location, and it being moved to a different location.

of the Kim Engineering Building (KEB) at the University of Maryland, College Park. The trajectory followed by the recorder can be seen in Figure 6(a). Each number denotes a 2-minute stop made by the recorder. In most of the cases, a stop is equivalent to the recorder being placed in one location in a room/corridor. However, in the case of stops 10-15 and 16-21, we have placed the recorder in 6 different locations in two different rooms, Rm 2111 and Rm 2107, respectively. This was done in an effort to further examine how the specific location within an environment can have an effect on the presence of ENF traces.

Figure 6(b) shows the spectrogram strips about the ENF harmonics for the hour long audio signal. The numbers in Figure 6(b) denote the stop where the recorder was stationed while that portion of the recording was being made. From this figure, we can see that there are three major harmonics around which the ENF traces are appearing strongly: 120 Hz, 240 Hz, and 360 Hz. We also note that, in between stops as the recorder is being moved from one stop to another, there is significant noise and no dominant ENF traces can be observed. This is similar to the observations seen in Section III-B.

We can visibly see that the strength of the ENF component can vary from one recording location to another. The 360 Hz

component, in particular, seems to be strong in only a handful of locations, such as locations 4, 7, and 8, and almost non-existent in others, such as in locations 16-21. To explain this, we can note that all these different rooms/corridors contain different equipment that emit different audio signals carrying ENF traces. Also, some differences can be attributed to constructive/destructive interferences among the signals carrying ENF traces. An indication of this is that location 10 has a visibly weaker 240 Hz component than the rest of the locations 11-15 in the same room.

To assess how well the ENF traces are captured at each location, we examine the correlation coefficient between the ENF signal extracted from an audio clip around a certain harmonic with the reference ENF signal extracted from the corresponding reference power clip. A high correlation coefficient value would indicate that ENF traces were embedded strongly at the harmonic in question in the audio recording, and consequently, the extracted ENF signal matches well with the reference power ENF signal. For this set of recordings, we extracted ENF signals for frames of 10-seconds long with 50 % overlap using an STFT-based ENF estimation approach.

Figure 7 shows the correlation coefficient values obtained for all the locations considered for the cases of ENF signals

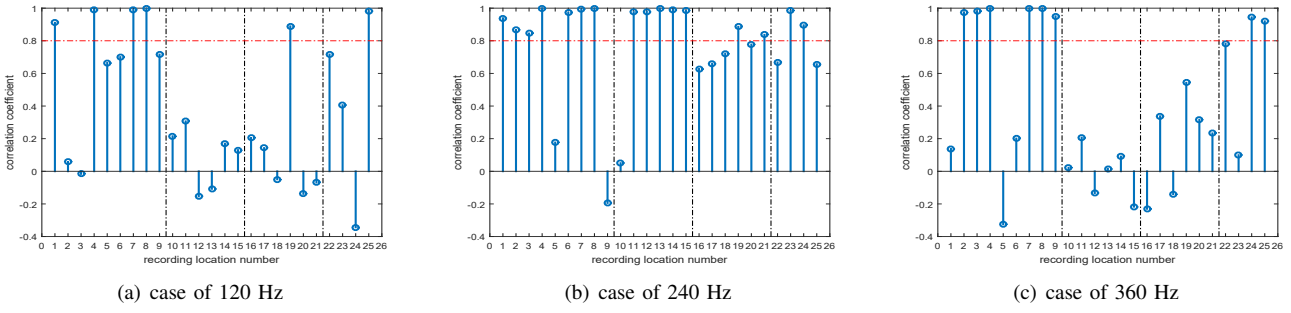


Fig. 7. Correlation coefficient values obtained for all the location cases considered for ENF signals extracted from around solely either the 120 Hz, 240 Hz, or 360 Hz harmonic. Each correlation coefficient value is computed between an extracted ENF signal about an ENF harmonic with its corresponding reference power ENF signal segment. Vertical black borders are placed around locations of recording that belong to the same room, i.e., locations 10-15 and locations 16-21, respectively.

extracted solely from around the 120 Hz, the 240 Hz, or the 360 Hz harmonic. The red horizontal line refers to a 0.8 correlation coefficient value, which we have empirically chosen as the lower bound for an acceptably high correlation coefficient value. Recording clips achieving lower than this value are considered to have either not captured ENF traces at the particular harmonic or captured them weakly.

Examining Figure 6(b), we can see that there is a strong component at 120 Hz throughout locations 10-21, even though this does not reflect in high correlation coefficients in most of these locations in Figure 7(a). It would seem that this component, which visibly seems to exhibit a high local SNR is not the ENF component and could be the result of stray electromagnetic spectra in the location of recording. For the case of the 120 Hz component in Figure 7(a), we can see that the only locations that give a high correlation coefficient are 1, 4, 7, 8, 19, and 25. Location 19 is the sole location in Rm 2107 to show prominent ENF at 120 Hz.

Examining Figure 7(b), we can see that most of the clips show high correlation coefficient values for the 240 Hz ENF component, thus exhibiting strong ENF traces. Again, we see another example of a sole recording in one room that does not exhibit similar behavior as the rest, i.e., location 10 in Rm 2111. This confirms our earlier observation that the 240 Hz component was captured weakly at location 10 and strongly at locations 11-15.

Examining Figure 7(c) confirms our earlier observation that the 360 Hz ENF component is strong at locations 4, 7, and 8. We can also see that the visibly faint 360 Hz components at locations 2, 3, 9, 24, and 25 in Figure 6(b) were enough in these cases to yield good ENF signal estimates.

The results shown in this section provide further evidence that the environment and the specific location within it in which a recording is made can have an effect on the strengths and harmonic locations of captured ENF traces.

IV. EXPLORATIONS ON DEVICE-RELATED FACTORS

In this section, we show results of experiments that suggest that the recorder (receiver) used to make an audio recording can have an effect on the way ENF traces are captured in the resulting recording. As discussed earlier, ENF traces are not restricted to appear in the frequency band surrounding

the nominal 50/60 Hz band, but can also appear in bands surrounding the harmonics of the nominal ENF value. As such, when examining whether ENF traces are present in a recording, we examine frequency bands surrounding not only the nominal ENF value, but its harmonics as well.

In the experiments that follow, we concurrently record a reference power recording while carrying out audio recordings. We examine the spectrogram strips about the ENF harmonics of the audio signal to identify if ENF traces were captured. To confirm that the traces observed were indeed due to the ENF, and not due to some other possible environmental signals, we compare the audio ENF variations to the ENF variations observed in the concurrently made power recordings. It is through this approach that we can confirm that the traces found about the ENF harmonics for the recordings shown in this section were indeed due to the ENF signal. Following this, the metric that we used to judge the strength of ENF presence in this section was a weight that estimates the local SNR at each ENF harmonic. We explain how we arrive at this estimate in Section IV-A. Then, we show the results of our experiments on device-related factors in Section IV-B.

A. Computation of local SNR estimate

ENF traces will appear in an audio recording when a signal carrying these traces is captured in it, e.g., the acoustic mains hum. We can express this signal as a summation of k sinusoids, each with an amplitude A_k , and whose frequency is time-varying around a harmonic of the nominal ENF value. Here, we aim to obtain an estimate of the local SNR at particular ENF harmonics, expressed in deciBels (dB). We denote the local SNR at the k^{th} harmonic by:

$$SNR_k = 10 \log \frac{P_{\text{signal},k}}{P_{\text{noise},k}} = 10 \log \frac{A_k^2}{P_{\text{noise},k}}, \quad (2)$$

where $P_{\text{signal},k}$ and $P_{\text{noise},k}$ are the powers of the signal and noise components, respectively, at the k^{th} harmonic.

To estimate the SNR of a certain ENF component contained in a signal, we examine the spectrogram of the audio signal, which gives estimates of the power spectral density (PSD) at different frequencies over time. We first divide the signal into consecutive frames, each on the order of a few seconds. For each frame, we find the PSD value of the peak of the

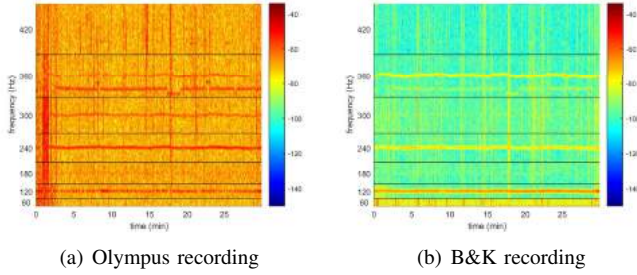


Fig. 8. Spectrogram strips about the harmonics of 60 Hz from the first set of simultaneously recorded audio measurements in the same environment made by Olympus and B&K recorders.

TABLE III
SNR ESTIMATES (IN dB) IN SET OF SIMULTANEOUS RECORDINGS MADE BY DIFFERENT RECORDERS, OLYMPUS AND B&K, IN THE SAME SETTING

SNR around	Set 1		Set 2		Set 3	
	Olym.	B&K	Olym.	B&K	Olym.	B&K
120 Hz	8.39	26.41	18.47	23.23	19.23	26.47
240 Hz	11.86	17.34	8.85	14.17	8.92	12.80
360 Hz	6.93	15.61	6.93	7.07	14.25	20.79

spectrogram surrounding the multiple of the nominal ENF value we are interested in; this is our estimate of $P_{S+N,k} = P_{signal,k} + P_{noise,k}$ as it corresponds to the signal peak superimposed over the noise present. Denoting the frequency at which this peak appears as $f_{peak,k}$, we compute our estimate for $P_{noise,k}$ as the average of the PSD values corresponding to the frequencies in the ranges of $[f_{peak,k} - \Delta_1, f_{peak,k} - \Delta_2]$ and $[f_{peak,k} + \Delta_2, f_{peak,k} + \Delta_1]$. For the experiments shown here, we have empirically chosen $\Delta_1 = 2$ Hz and $\Delta_2 = 0.5$ Hz. This choice was made after many observations of the behavior of the ENF in the grid where we made our recordings, the Eastern US grid; these values would need to be larger if the recordings were being made in grids where the ENF has larger range of variations, such as in India or Lebanon [7]. After computing the $P_{signal,k}$ estimate as $P_{S+N,k} - P_{noise,k}$, we can compute the SNR_k estimate using Equation (2). Through this approach, we can estimate the SNR_k value for each frame. We can also compute the average SNR_k value over a certain time period as the mean of the SNR_k values of the frames within this time period.

B. Experiments and Results

In what follows, we present the results of three experiments that we carried out, which suggest that the recording device used can have an effect on (i) the strength by which ENF traces are captured in a recording, and (ii) the ENF harmonics around which the traces can appear. The experiments discussed here were carried out at the University of Maryland, where the nominal ENF value is 60 Hz.

1) *Difference in ENF strength:* In this experiment, we carry out three sets of simultaneous recordings by two different receivers. Each recording is 30 minutes long. The first receiver is the built-in microphone of the Olympus 700-M audio

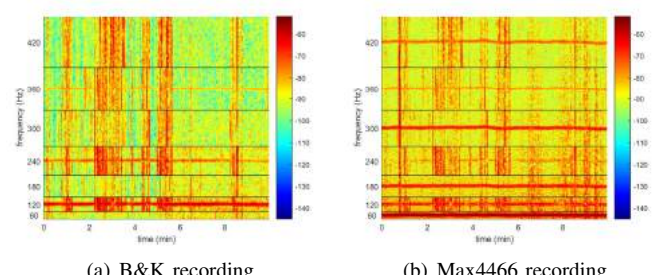


Fig. 9. Spectrogram strips about the harmonics of 60 Hz from the set of simultaneously recorded audio measurements in the same environment made by B&K and Max4466 recorders.

TABLE IV
SNR ESTIMATES (IN dB) IN SET OF SIMULTANEOUS RECORDINGS MADE BY DIFFERENT RECORDERS, B&K AND MAX4466, IN THE SAME SETTING

SNR around	B&K	Max4466
60 Hz	5.10	19.05
120 Hz	16.44	9.67
180 Hz	3.75	16.22
240 Hz	10.46	5.61
300 Hz	3.65	18.38
360 Hz	9.58	8.73
420 Hz	3.64	12.61

recorder [26], and the second receiver is a Brüel & Kjær (B&K) microphone (type 2669) [29]. Figure 8 shows spectrogram strips of the recordings surrounding ENF harmonics for one set of the recordings. Here, we can see that both recorders capture prominent ENF traces at around 120 Hz and 240 Hz, and the B&K recording additionally captures strong ENF traces at around 360 Hz.

When comparing the 240 Hz strips between the two spectrograms in Figure 8, we can see that the ENF traces captured by the Olympus recorder have a red color while those of the B&K recording have a yellow color. Examining the color bars of the spectrograms indicates that the Olympus recording's strip has a higher PSD value than that of the B&K recording. However, a more telling indicator on the strength of the captured ENF traces is their respective local SNR estimated following Section IV-A.

We compute the SNR estimates around 120 Hz, 240 Hz, and 360 Hz using the approach described earlier. The results, shown in Table III, show that for each of these ENF components present in the audio signals, the component in the B&K recording has a higher SNR estimate than its counterpart in the Olympus recording.

Given that each set of recordings was made in the same location, this suggests that using the B&K would yield stronger ENF traces, demonstrating that the choice of receiver can have an effect on the strength by which the ENF traces are captured.

2) *Difference in ENF harmonics captured:* In this experiment, we carry out two simultaneous audio recordings using different receivers in the same environment. Here, one of the receivers is the B&K microphone used in the experiments of Section IV-B1, and the second receiver is a Max4466 microphone from Adafruit [30]. Figure 9 shows the spectrogram

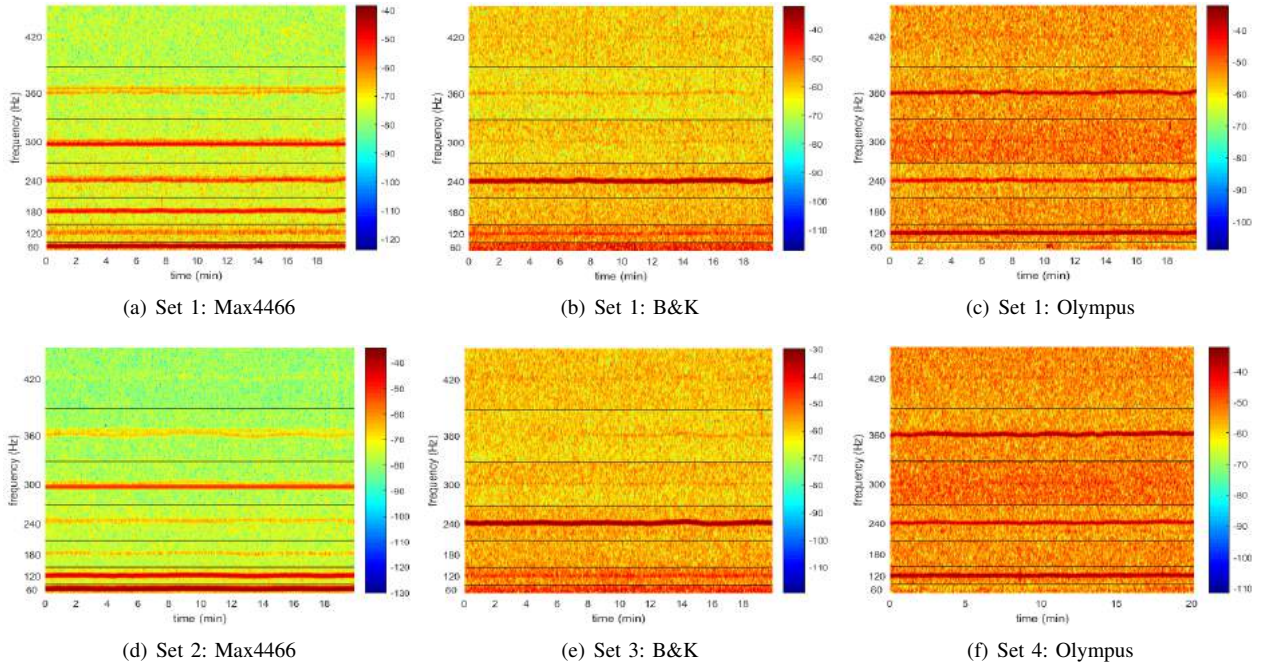


Fig. 10. Spectrogram strips about the harmonics of 60 Hz from the set of simultaneously recorded audio measurements in the same environment made by different recorders, B&K and Max4466.

strips about the ENF harmonics for the recordings made.

The results of this experiment yield an interesting observation: Even though both recordings were made in the same location, the B&K microphone captures the ENF traces at even harmonics of 60 Hz, which is consistent with the results of Section IV-B1, while the Max4466 captures the ENF traces at odd harmonics of 60 Hz. For reference, Table IV also shows the SNR estimates computed for the ENF traces observed in the recordings to give a numerical perspective on the local strengths of the ENF traces. These results suggest that the choice of recorder can have an effect on the ENF harmonic at which ENF traces appear.

3) *Further examination:* The results of the first experiment suggest that the microphone (receiver) used can have an effect on the strength of the ENF traces captured in an audio recording, whereas the results of the second experiment suggest that the microphone (receiver) used can have an effect on the frequencies at which ENF traces appear. One phenomenon that could have played a part in the previous results is that of interference between the two microphones being used at the same time. To be able to examine whether that phenomenon does play a factor or not, and to get further datapoints to support or negate our previous results, we have carried out this third round of experiments, which aims to look at the recordings made by each of the three microphones examined (Olympus, B&K and Max4466) when no other recorder is being used at the same time. This third round of experiments is formed of four sets:

- Set 1: Recordings using all three microphones (Olympus, B&K and Max4466).
- Set 2: Recording using only the Max4466 microphone.
- Set 3: Recording using only the B&K microphone.

- Set 4: Recording using only the Olympus microphone.

All of the sets of recordings carried out were made for 20-minutes intervals in the same room on the campus of the University of Maryland. Each set was supported by a concurrent reference power recording. As in previous cases, the power recording was used to validate that traces found in audio recordings at harmonics of the nominal ENF were indeed due to the ENF variations, and not due to other electromagnetic spectra in the recording environment.

Figure 10 shows the spectrograms of the audio signals recorded in this round of experiments. We are also including the ENF estimates extracted from around the visible spectrogram strips seen for each of the audio recordings for Set 1, shown along with the ENF signal extracted from the concurrently made reference power recording. These signals are shown in Figures 11, 12, and 13. We can examine this plots to notice that if the trend of variation of the audio ENF matches that of the power ENF, this would verify that the observed traces are due to ENF.

From Figure 11, we can see that the ENF traces are captured in the Max4466 recording at 60 Hz, 180 Hz, 240 Hz, and 360 Hz, and not at 120 Hz or 300 Hz despite the suggestive strong frequency bands appearing in the spectrogram of Figure 10(a). When doing a similar analysis for the Max4466 recording of Set 2, we found that it captured ENF traces at 60 Hz, 120 Hz, 180 Hz, and 360 Hz, but not at 240 Hz or 300 Hz. Although the difference between the two cases here is whether or not ENF traces were captured at 120 Hz or 240 Hz, an interesting observation remains consistent. That is, the Max4466 was the only recorder we observed to capture ENF traces at the odd harmonics 60 Hz and 180 Hz.

From Figure 12, we can see that the ENF traces were

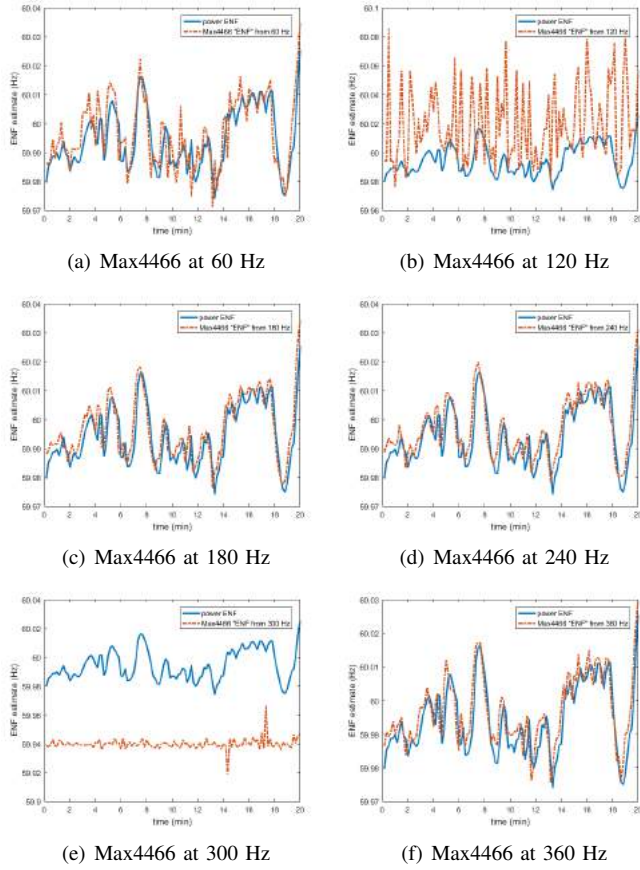


Fig. 11. ENF estimates extracted from Max4466 recordings from around different ENF harmonics, shown along with ENF signal estimated from concurrently made power recording.

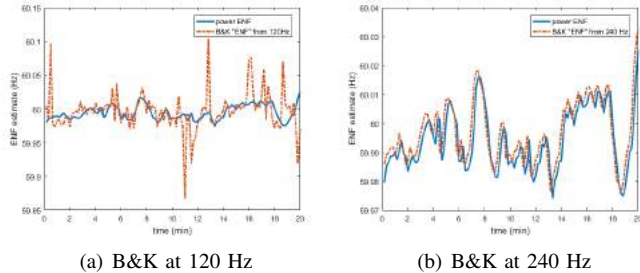


Fig. 12. ENF estimates extracted from B&K recordings from around different ENF harmonics, shown along with ENF signal estimated from concurrently made power recording.

captured in the B&K recordings at 120 Hz and 240 Hz, though more strongly at 240 Hz. From Figure 13, we can see the Olympus recorder captured ENF traces at 120 Hz, 240 Hz, and 360 Hz. Similar observations were also made when examining the ENF estimates extracted from the B&K and Olympus recordings from Sets 3 and 4, respectively.

From Figure 10, we can see that each microphone exhibits similar behavior when combined with other recordings (Set 1) and when in a set by itself (Sets 2, 3, and 4): Max4466 shows ENF traces at both even and odd harmonics of the nominal ENF value, and the other two recorders show ENF

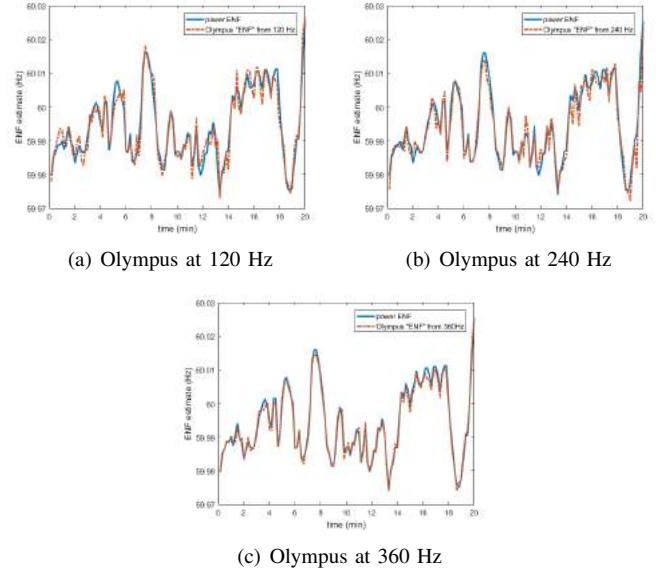


Fig. 13. ENF estimates extracted from Olympus recordings from around different ENF harmonics, shown along with ENF signal estimated from concurrently made power recording.

traces at even harmonics. This suggests that the observations made in Sections IV-B1 and IV-B2 are due to the microphone's individual characteristics and not due to interference between microphones. This is in agreement with results shown previously in that each microphone captures ENF traces at different harmonics, and Max4466 is notable in being the only microphone in our set of microphones examined that captures ENF traces on the odd harmonics.

4) Discussion: In each of the experiments shown in this section, we have used different recorders in the same environment to record the background noise carrying ENF traces. Examining the results of these experiments, we can hypothesize that the choice of recorder used to make an audio recording can influence the strength of the ENF traces captured and the harmonic locations at which these ENF traces appear.

In Section III, however, we have seen that the specific locations within an environment where an audio recorder is placed can have an effect as well on the strengths/locations by which ENF traces are captured in the resulting recording. It is therefore plausible that such factors may have played a role as well in the results shown in this section, in addition to factors related to the recorders being used. This demonstrates that the mechanisms and influencing factors about how ENF traces are captured in a recording are complex problems, and it will need further study to achieve a comprehensive understanding.

V. CONCLUSION AND FUTURE WORK

The ENF signal has been under study in the community in recent years for its ubiquitous nature as it can be captured intrinsically by media recordings. Research work has been carried out to propose approaches to extract it and explore its subsequently interesting applications in information forensics and security. There is a need, however, for further research into the factors and conditions that can promote or hinder the

capture of ENF traces in media recordings. This would help us gain a stronger understanding on the situations where the use of the ENF signal can be applicable, and could possibly help us design certain protocols that can increase the likelihood of the capture of ENF traces in recordings.

Through the study shown in this paper, we have seen that the choice of recorder used to make a recording can have an effect on the actual harmonics at which ENF traces appear, and on the strength by which ENF traces are captured. Factors related to the environment also play a role: the presence of different sources of waves carrying ENF traces and the interference between these waves and their reflected versions can affect the strength of the captured ENF traces at specific locations, and moving the recorder while making a recording can compromise the captured ENF traces.

We have seen in this study that understanding the factors that affect the capture of ENF traces in recordings is not a straightforward problem, as more than one factor would likely be contributing to the final state of the captured ENF traces. In the future, it would be beneficial to examine factors such as those explored in this paper, and others, in extensive and controlled experiments with respect to multiple factors, in a variety of locations and using different recorders including smartphone recorders heavily used today. A small-scale study that we have carried out suggests that ENF traces can be captured by the recorders built-in to iPhone and Android smartphones, and that the way the ENF traces are captured also varies across the locations and devices used. More systematic studies on cellphone recordings would help strengthen the understanding of the situations that promote or hinder the capture of ENF traces and ultimately better understand the real-world applicability of the ENF signal. A similar study can be done with video recordings as well where the role of factors such as internal video camera operations and the behavior of light waves in an environment can be explored. This will improve fundamental understandings on ENF based forensics analysis and complement such practical strategies that explore static regions [16], [31], [32] or perform motion compensation [19].

REFERENCES

- [1] M. H. J. Bollen and I. Y. H. Gu, *Signal Processing of Power Quality Disturbances*. Wiley-IEEE Press, 2006.
- [2] C. Grigoras, “Applications of ENF analysis in forensic authentication of digital audio and video recordings,” *J. Audio Eng. Soc*, vol. 57, no. 9, pp. 643–661, 2009.
- [3] O. Ojouo, J. Karlsson, J. Li, and Y. Liu, “ENF extraction from digital recordings using adaptive techniques and frequency tracking,” *IEEE Trans. on Info. Forensics and Security*, vol. 7, no. 4, Aug. 2012.
- [4] A. Hajj-Ahmad, R. Garg, and M. Wu, “Instantaneous frequency estimation and localization for ENF signals,” in *Asia-Pacific Signal Info. Proc. Association Annual Summit and Conf. (APSIPA ASC)*, Dec. 2012, pp. 1–10.
- [5] D. P. N. Rodríguez, J. A. Apolinário, and L. W. P. Biscainho, “Audio authenticity: Detecting ENF discontinuity with high precision phase analysis,” *IEEE Trans. on Info. Forensics and Security*, vol. 5, no. 3.
- [6] R. Garg, A. Hajj-Ahmad, and M. Wu, “Geo-location estimation from electrical network frequency signals,” in *IEEE Int. Conf. on Acoustics, Speech and Signal Processing (ICASSP)*, May 2013, pp. 2862–2866.
- [7] A. Hajj-Ahmad, R. Garg, and M. Wu, “ENF-based region-of-recording identification for media signals,” *IEEE Trans. on Info. Forensics and Security*, vol. 10, no. 6, pp. 1125–1136, June 2015.
- [8] G. Hua, Y. Zhang, J. Goh, and V. L. L. Thing, “Audio authentication by exploring the absolute-error-map of enf signals,” *IEEE Transactions on Information Forensics and Security*, vol. 11, no. 5, pp. 1003–1016, May 2016.
- [9] W. Yao, J. Zhao, M. J. Till, S. You, Y. Liu, Y. Cui, and Y. Liu, “Source location identification of distribution-level electric network frequency signals at multiple geographic scales,” *IEEE Access*, vol. 5, pp. 11 166–11 175, 2017.
- [10] G. Hua, G. Bi, and V. L. L. Thing, “On practical issues of electric network frequency based audio forensics,” *IEEE Access*, vol. 5, pp. 20 640–20 651, 2017.
- [11] D. Bykhovsky and A. Cohen, “Electrical network frequency (ENF) maximum-likelihood estimation via a multitone harmonic model,” *IEEE Trans. on Info. Forensics and Security*, vol. 8, no. 5, pp. 744–753, May 2013.
- [12] A. Hajj-Ahmad, R. Garg, and M. Wu, “Spectrum combining for ENF signal estimation,” *IEEE Signal Processing Letters*, vol. 20, no. 9, pp. 885–888, Sept. 2013.
- [13] L. Fu, P. N. Markham, R. W. Connors, and Y. Liu, “An improved discrete fourier transform-based algorithm for electric network frequency extraction,” *IEEE Trans. on Info. Forensics and Security*, vol. 8, no. 7, pp. 1173–1181, July 2013.
- [14] H. Su, A. Hajj-Ahmad, R. Garg, and M. Wu, “Exploiting rolling shutter for ENF signal extraction from video,” in *IEEE Int. Conf. on Image Processing (ICIP)*, Oct. 2014, pp. 5367–5371.
- [15] L. Dosiek, “Extracting electrical network frequency from digital recordings using frequency demodulation,” *IEEE Signal Processing Letters*, vol. 22, no. 6, pp. 691–695, June 2015.
- [16] S. Vatansever, A. E. Dirik, and N. Memon, “Detecting the presence of ENF signal in digital videos: A superpixel-based approach,” *IEEE Signal Processing Letters*, vol. 24, no. 10, pp. 1463–1467, Oct 2017.
- [17] Y. Zhang, P. Markham, T. Xia, L. Chen, Y. Ye, Z. Wu, Z. Yuan, L. Wang, J. Bank, J. Burgett, R. W. Connors, and Y. Liu, “Wide-area frequency monitoring network (FNET) architecture and applications,” *IEEE Trans. on Smart Grid*, vol. 1, no. 2, pp. 159–167, Sept. 2010.
- [18] P. A. Andrade Esquef, J. A. Apolinário, and L. W. P. Biscainho, “Edit detection in speech recordings via instantaneous electric network frequency variations,” *IEEE Trans. on Info. Forensics and Security*, vol. 9, no. 12, pp. 2314–2326, Dec. 2014.
- [19] H. Su, A. Hajj-Ahmad, C.-W. Wong, R. Garg, and M. Wu, “ENF signal induced by power grid: A new modality for video synchronization,” in *Proceedings of the 2nd ACM Int. Workshop on Immersive Media Experiences*. New York, NY, USA: ACM, Immersive Me, 2014, pp. 13–18.
- [20] L. Cuccovillo and P. Aichroth, “Increasing the temporal resolution of enf analysis via harmonic distortion,” in *AES Int. Conf. on Audio Forensics*, June 2017. [Online]. Available: <http://www.aes.org/e-lib/browse.cfm?lib=18736>
- [21] N. Fechner and M. Kirchner, “The humming hum: Background noise as a carrier of ENF artifacts in mobile device audio recordings,” in *2014 8th Int. Conf. on IT Security Incident Management IT Forensics (IMF)*, May 2014, pp. 3–13.
- [22] E. B. Brixen, “Techniques for the authentication of digital audio recordings,” in *Audio Engineering Society Convention 122*, May 2007.
- [23] J. Chai, F. Liu, Z. Yuan, R. W. Connors, and Y. Liu, “Source of enf in battery-powered digital recordings,” in *Audio Engineering Society Convention 135*, Oct 2013. [Online]. Available: <http://www.aes.org/e-lib/browse.cfm?lib=17055>
- [24] “Sound Waves and Music,” [Online]. Available: <http://www.physicsclassroom.com/class/sound/>. Accessed: June 2016.
- [25] “The Doppler Effect and Sound Interference – Scientific Sofia,” [Online]. Available: <http://dropdeadsofia.weebly.com/the-doppler-effect-and-sound-interference.html>. Accessed: Aug. 2016.
- [26] “Olympus Digital Voice Recorder Detailed Instructions,” [Online]. Available: http://www.olympusamerica.com/files/oima_ckb/ws-710m_ws-700m_ws-600s_instructions_en.pdf. Accessed: Aug. 2016.
- [27] “ENF: Power signature for information forensics,” [Online]. Available: <http://www.mast.umd.edu/index.php/enf-menu>, Media and Security Team (MAST), at the University of Maryland. Accessed: Oct. 2016.
- [28] “UMCP / Kim Engineering Building Floor Plan – Floor 2,” [Online]. Available: <https://apra.umd.edu/publicAccess/kim/floors.jsp?floor=2>. Accessed: July 2016.
- [29] “Brüel & Kjær – Company Homepage,” [Online]. Available: <http://www.bksv.com/>, accessed Aug. 2016.
- [30] “Electret Microphone Amplifier - MAX4466,” [Online]. Available: <https://www.adafruit.com/product/1063>, accessed Aug. 2016.

- [31] R. Garg, A. L. Varna, and M. Wu, "Seeing' ENF: Natural time stamp for digital video via optical sensing and signal processing," in *Proceedings of the 19th ACM Int. Conf. on Multimedia*.
- [32] R. Garg, A. Varna, A. Hajj-Ahmad, and M. Wu, "Seeing' ENF: Power-signature-based timestamp for digital multimedia via optical sensing and signal processing," *IEEE Trans. on Info. Forensics and Security*, vol. 8, no. 9, pp. 1417–1432, Sept 2013.



Adi Hajj-Ahmad (S10 - M17) received the B.E. degree in electrical and computer engineering from the American University of Beirut, Beirut, Lebanon, in 2011, and the M.S. and Ph.D. degrees in electrical engineering from the University of Maryland, College Park, in 2015 and 2016, respectively. He is currently a Senior Data Scientist with GE Digital in San Ramon, CA, where he works on addressing statistical, machine learning and data understanding problems for industrial customers in different industries. His research interests include signal processing, information forensics and machine learning.

Dr. Hajj-Ahmad has received the A. James Clark School of Engineering Distinguished Graduate Fellowship in 2011, the Distinguished Teaching Assistant Award in 2013, the Northrop Grumman Graduate Fellowship in Engineering Education in 2015, the Invention of the Year Award in 2015, and the Jimmy Lin Award for Innovation in 2016, all from the University of Maryland. His paper in the ACM Workshop on Information Hiding and Multimedia Security won the Best Student Paper Award in 2015. He was on the organizing team of the third edition of the IEEE Signal Processing Cup in 2016 on electric network frequency forensics.



Qiang Zhu (S'17) is a Ph.D. student in the Electrical and Computer Engineering Department at the University of Maryland (UMD), College Park. Before joining UMD, he received his B.E. degree in control science and engineering from Zhejiang University, Hangzhou, China, in 2010, and the M.S. degree in electrical information and electrical engineering from the Shanghai Jiao Tong University, Shanghai, China, in 2014. His research interests include signal processing, information forensics and machine learning.



Miao Yu received her B.S. and M.S. degrees in engineering mechanics from Tsinghua University in 1996 and 1998, respectively, and her Ph.D. degree in 2002 from the University of Maryland, College Park. Since 2005, she has been with the University of Maryland, College Park where she is currently a Professor and the director of the Sensors and Actuators Laboratory, dedicated to research on micro/nano sensors, photonics, and smart materials and structures.

Dr. Yu received the 2006 Oak Ridge Associated Universities Ralph E. Powe Junior Faculty Enhancement Award. In 2007, she was recognized with both the NSF CAREER Award and the Young Investigator Research Program Award from AFOSR for her work on biology inspired sensors. Dr. Yu holds 14 invention disclosures, six issued U.S. patents, and two U.S. patent applications. She received the University of Maryland Invention of the Year award in the category of Physical Sciences in 2002 and was a finalist in 2010 and 2011. She is currently an Associate Editor of the ASME Journal of Vibration and Acoustics. She was named an American Society of Mechanical Engineers (ASME) Fellow in 2017.



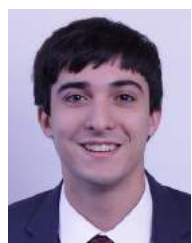
Chau-Wai Wong (S'05–M'16) received the B.Eng. degree with first class honors in 2008, and M.Phil. degree in 2010, both in electronic and information engineering from The Hong Kong Polytechnic University, and the Ph.D. degree in electrical and computer engineering from the University of Maryland, College Park in 2017. He worked as a Data Scientist at Origin Wireless, Inc. in 2017. He is currently an Assistant Professor at the Department of Department of Electrical and Computer Engineering, North Carolina State University. His research interests include multimedia forensics, statistical signal processing, data analytics, and video coding.

Dr. Wong received the University of Maryland Future Faculty Fellowship, HSBC Scholarship, Hitachi Scholarship, Chinese Government Award for Outstanding Students Abroad, and two-year and four-year merit-based full scholarships for M.Phil. and B.Eng. studies, respectively. He was a co-recipient of a Top-4 Student Paper Award from the public relations division at the 67th Annual Conference of International Communication Association. He is a member of the IEEE and the APSIPA, and he was the general secretary of the IEEE PolyU Student Branch from 2006 to 2007. He was involved in organizing the third edition of the IEEE Signal Processing Cup in 2016 on electric network frequency forensics.



Min Wu (S'95–M'01–SM'06–F'11) received the B.E. degree in electrical engineering and the B.A. degree in economics from Tsinghua University in Beijing, China (both with the highest honors), in 1996, and the Ph.D. degree in electrical engineering from Princeton University in 2001. Since 2001, she has been with University of Maryland, College Park, where she is currently a Professor and a University Distinguished Scholar-Teacher. She leads the Media and Security Team (MAST) at the University of Maryland, with main research interests on information security and forensics and multimedia signal processing.

Dr. Wu is a corecipient of two Best Paper Awards from the IEEE Signal Processing Society and EURASIP, respectively. She also received an NSF CAREER award in 2002, a TR100 Young Innovator Award from the MIT Technology Review Magazine in 2004, an ONR Young Investigator Award in 2005, a ComputerWorld "40 Under 40 IT" Innovator Award in 2007, an IEEE Mac Van Valkenburg Early Career Teaching Award in 2009, and an IEEE Distinguished Lecturer recognition for 2015–2016. She has served as Vice President-Finance of the IEEE Signal Processing Society (2010–2012), Chair of the IEEE Technical Committee on Information Forensics and Security (2012–2013), and Editor in Chief of the IEEE SIGNAL PROCESSING MAGAZINE (2015–2017). She was elected IEEE Fellow and AAAS Fellow for contributions to signal processing, multimedia security and forensics.



Steven Gambino received a B.S. degree in mechanical engineering and an M.E. degree in robotics in 2016 and 2018, respectively, both from the University of Maryland, College Park. His research interests include signal processing, machine learning, and autonomous vehicles. He worked in Prof. Miao Yu's Sensors and Actuators Lab from 2015 to 2017.